Cell Cycle 9:22, 4518-4524; November 15, 2010; © 2010 Landes Bioscience

Vessel destruction by tumor-targeting *Salmonella typhimurium* A1-R is enhanced by high tumor vascularity

Fang Liu,[1-3] Lei Zhang,[1,2] Robert M. Hoffman[1,2,*] and Ming Zhao[1]

[1]AntiCancer Inc.; San Diego, CA; [2]Department of Surgery; University of California at San Diego; San Diego, CA USA; [3]Dept of Anatomy; Second Military Medical University; Shanghai, China

Key words: tumor targeting bacteria, *Salmonella typhimurium* A1-R, Lewis lung carcinoma, RFP, GFP, nestin, nude mice

Our laboratory has previously developed a tumor-targeting double-auxotrophic mutant of *Salmonella typhimurium* termed A1-R. The present report demonstrates that *S. typhimurium* A1-R destroys tumor blood vessels and this is enhanced in tumors with high vascularity. Red fluorescent protein (RFP)-expressing Lewis lung cancer cells (LLC-RFP) were transplanted subcutaneously in the ear, back skin and footpad of nestin-driven green fluorescent protein (ND-GFP) transgenic nude mice, which selectively express GFP in nascent blood vessels. Color-coded in vivo imaging demonstrated that the LLC-RFP ear tumor had the highest cell density and the footpad tumor had the least. The ear tumor had more abundant blood vessels than that on the back or footpad. The tumor-bearing mice were treated with A1-R bacteria via tail-vein injection. Tumors in the ear were the earliest responders to bacterial therapy and hemorrhaged severely the day after A1-R administration. Tumors growing in the back were the second fastest responders to bacterial treatment and appeared necrotic 3 days after A1-R administration. Tumors growing in the footpad had the least vascularity and were the last responders to A1-R. Therefore, tumor vascularity correlated positively with tumor efficacy of A1-R. The present study suggests that bacteria efficacy on tumors involves vessel destruction which depends on the extent of vascularity of the tumor.

Introduction

Coley[1] observed, more than a century ago, that some cancer patients were cured of their tumors following postoperative bacterial infection. In the middle of the last century, Malmgren and Flanigan[2] showed that anaerobic bacteria had the ability to survive and replicate in necrotic tumor tissue with low oxygen content. Several approaches aimed at utilizing bacteria for cancer therapy have subsequently been described.[3-15]

Bifidobacterium longum has been shown to selectively grow in hypoxic regions of tumors following intravenous administration. This effect was demonstrated in 7,12-dimethylbenzanthracene-induced rat mammary tumors by Yazawa et al.[14,15]

Vogelstein et al. created a strain of *Clostridium novyi*, an obligate anaerobe, which was depleted of its lethal toxin.[16] This strain of *C. novyi* was termed *C. novyi* NT. Following intravenous administration, the *C. novyi* NT spores germinated in the avascular regions of tumors in mice, causing damage to the surrounding viable tumor.[16] Combined with conventional chemotherapy or radiotherapy, intravenous *C. novyi* NT spores caused extensive tumor damage within 24 h.[16]

Following attenuation by purine and other auxotrophic mutations, the facultative anaerobe *Salmonella typhimurium* was used for cancer therapy.[11,17,18] These genetically modified bacteria replicated in tumors to levels more than 1,000-fold greater than in normal tissue.[11] *S. typhimurium* was further modified genetically by disrupting the msbB gene to reduce the incidence of septic shock.[11]

The msbB mutant of *S. typhimurium* has been tested in a Phase I clinical trial to determine its efficacy on metastatic melanoma.[19] To raise the therapeutic index, *S. typhimurium* was further attenuated by deletion of the purI as well as msbB gene.[19] The new strain of *S. typhimurium*, termed VNP20009, could then be safely administered to patients.[19] More studies are needed to completely characterize the safety and efficacy of these bacteria and to improve its therapeutic index.

Mengesha et al. utilized *S. typhimurium* as a vector for gene delivery by developing a hypoxia-inducible promoter (HIP-1) to limit gene expression to hypoxic tumors. HIP-1 was able to drive gene expression in bacteria infecting human tumor xenografts implanted in mice. Genes linked to the HIP-1 promoter showed selective expression in tumors.[20]

*Correspondence to: Robert M. Hoffman; Email: all@anticancer.com
Submitted: 08/25/10; Accepted: 09/24/10
Previously published online: www.landesbioscience.com/journals/cc/article/13744
DOI: 10.4161/cc.9.22.13744

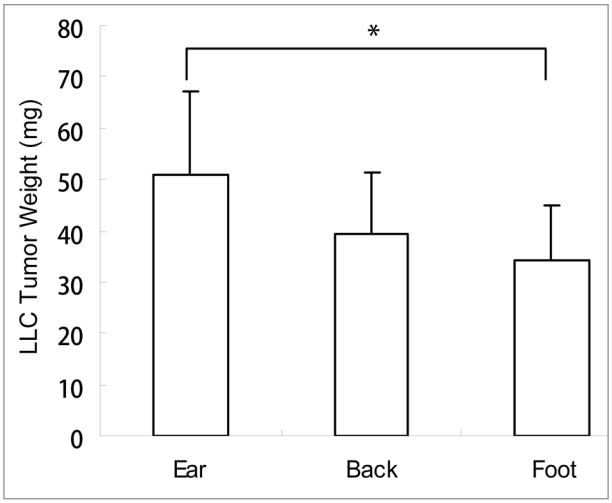

Figure 1. Weight of the Lewis lung tumor at different body sites. Lewis lung tumor cells were injected subcutaneously into the ear, back and footpad at a cell density of 2 x 10^7/ml, using a 25 μl cell suspension at each site. 10 days after tumor growth, the tumors were taken out and weighed individually. Average tumor weight was obtained. Weight of the ear tumor was larger than that in the back or foot. A significant difference was found between the tumor in the ear and the footpad. *p < 0.05 ear tumor vs. footpad tumor.

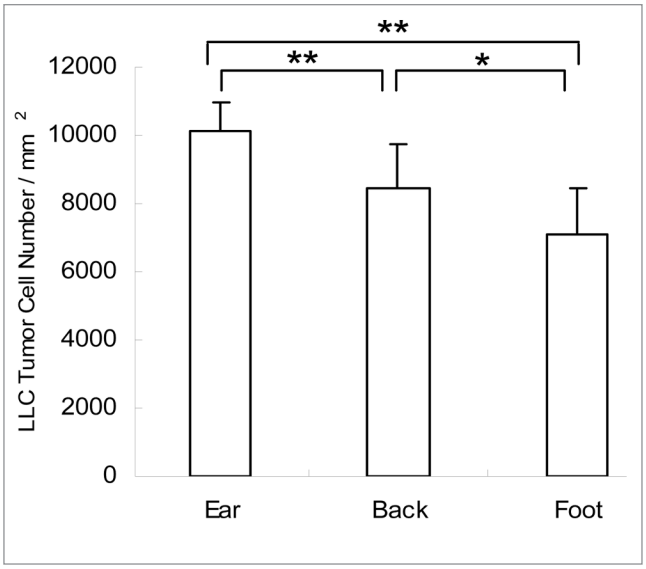

Figure 2. Density of the Lewis lung tumor cells at different body sites. Cell numbers were counted in ten random areas (1 mm^2 each) at each site using paraffin sections. The average tumor cell number per mm^2 at different sites was obtained and compared. Tumor cell density in the ear was higher than that in the back or footpad. Tumor cell density in the back was also higher than that in the foot. **p < 0.01, ear tumor vs. back and foot tumor; *p < 0.05 back tumor vs. foot tumor.

Yu et al. used green fluorescent protein (GFP)-labeled bacteria to visualize tumor targeting abilities of three pathogens: *Vibrio cholerae*, *S. typhimurium* and *Listeria monocytogenes*.[21,22]

We have developed an effective bacterial cancer therapy strategy by targeting viable tumor tissue using *Salmonella typhimurium* auxotrophs that we have generated which grow in viable as well as necrotic areas of tumors. Importantly, the auxotrophy severely restricts growth of these bacteria in normal tissue. In vitro, A1-R infects tumor cells and causes nuclear destruction.[23] A1-R was initially used to treat metastatic human prostate and breast tumors that had been orthotopically implanted in nude mice.[24] A1-R administered i.v. to nude mice with primary osteosarcoma and lung metastasis was highly effective, especially against metastasis.[25] A1-R was also targeted to both axillary lymph and popliteal lymph node metastasis of human pancreatic cancer and fibrosarcoma, respectively, as well as lung metastasis of the fibrosarcoma in nude mice.[26] A1-R was administered intratumorally to nude mice with an orthotopically transplanted human pancreatic tumor. The primary pancreatic cancer regressed without additional chemotherapy or any other treatment.[27] A1-R was also effective against pancreatic cancer liver metastasis when administered intrasplenically to nude mice.[28]

Leschner et al. have observed a large influx of blood into the tumors by vascular disruption after treatment with *S. typhimurium*. Blood influx was followed by necrosis formation.[29]

We have utilized multicolored fluorescent proteins to develop imaging models of tumor angiogenesis. We have used a transgenic mouse in which the regulatory elements of the stem cell marker nestin drives GFP (ND-GFP). The ND-GFP mouse expresses GFP in nascent blood vessels. RFP-expressing tumors transplanted to nestin-GFP mice enable specific visualization of nascent vessels.[30,31]

The present study utilizes the ND-GFP mouse model implanted with the Lewis lung carcinoma at various sites, with color-coded imaging, and suggests that bacteria efficacy on tumors involved vessel destruction which is enhanced by high vascularity of the tumor.

Results

Tumor vascularity varies with tumor location. Tumors in the ear had the fastest growth rate as measured by tumor weight (**Fig. 1**) and tumor-cell density (**Fig. 2**). CD31-immnohistochemical staining of the tumor sections showed that the ear tumor also had the most abundant blood vessels (**Fig. 3**). Observation with the IV-100 imaging system also showed that blood vessels in the ear tumor were very dense and interwoven to form a blood vessel network (**Fig. 4B**). Tumors implanted in the back grew the second fastest (**Fig. 1**). Blood vessels in the back tumors also formed networks but were less dense than vessels in the ear tumor (**Fig. 5B**). Tumors in the footpad were the slowest growing (**Fig. 1**). More parallel blood vessels were observed in the foot tumor (**Fig. 6B**). Both the area and average grey values of the footpad tumor blood vessels were much less than vessels in the ear tumor ($p < 0.01$, **Figs. 7 and 8**).

Response to *S. typhimurium* A1-R bacteria correlates with tumor vascularity. Tumors in the ear were the earliest responders to A1-R bacteria and hemorrhaged severely one day after A1-R infection (**Fig. 4C and D**). Tumors growing in the back were the second fastest responders to A1-R and appeared necrotic three

days after A1-R infection (**Fig. 5E and F**). Tumors in the footpad were the least responsive to A1-R and obvious necrosis was observed six-days after A1-R treatment (**Fig. 6F**). Tumor vascularity correlated positively with A1-R efficacy with the ear being the most vascular site and the footpad the least vascular site.

Destruction of tumor blood vessels by *S. typhimurium* A1-R correlates with tumor vascularity. Blood vessels in the tumors in the ear were severely destroyed one day after A1-R bacteria infection. Blood vessels fragmented in most areas of the tumor. The blood vessel area greatly decreased by day 1 after A1-R bacteria treatment ($p < 0.05$). The average grey value of the blood vessels also decreased ($p < 0.01$). Only a few blood vessels remained at day 3 after treatment. Very few blood vessels were seen at day 6 with A1-R bacteria treatment (**Figs. 4, 7 and 8**).

Some of the blood vessels of the back tumors were damaged by day 1 after A1-R bacteria infection. Large areas of the blood vessel were destroyed at day 3 and day 6 after bacterial infection. The average grey value of the blood vessels decreased at day 3 ($p < 0.01$) and day 6 ($p < 0.01$).

Blood vessels of the foot tumor were destroyed at day 6 after bacteria infection. The area and average grey value of the tumor blood vessels were both much less than that in the control group (**Figs. 6–8**).

Discussion

In the present study, we found that the Lewis lung tumor had different growth rates at different body sites. The tumor cell density and distribution of blood vessels varied at different sites. The denser the tumor cells were, the richer the tumor blood vessels appeared. Response to A1-R bacteria varied at different sites. The results demonstrate that tumor vascularity correlated to tumor sensitivity to A1-R bacteria.

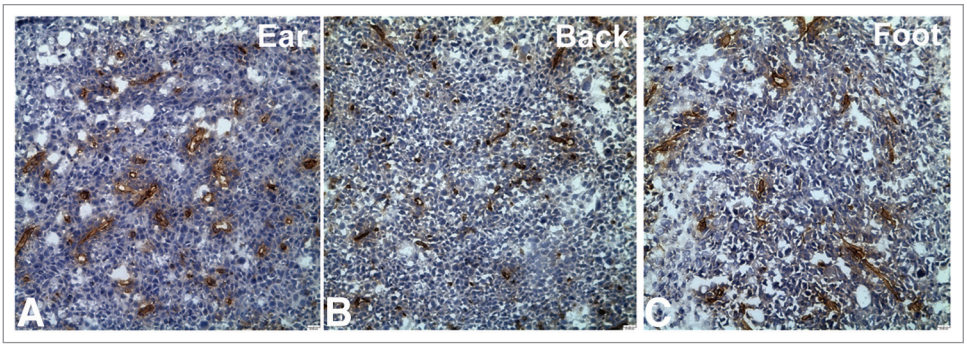

Figure 3. CD31-immunohistochemical staining of the Lewis lung tumor at different body sites. (A) Ear tumor; (B) Back tumor; (C) Foot tumor. CD31-positive staining is shown in brown. Sections were counter-stained with haematoxylin. Blood vessels in the ear tumor were the most abundant.

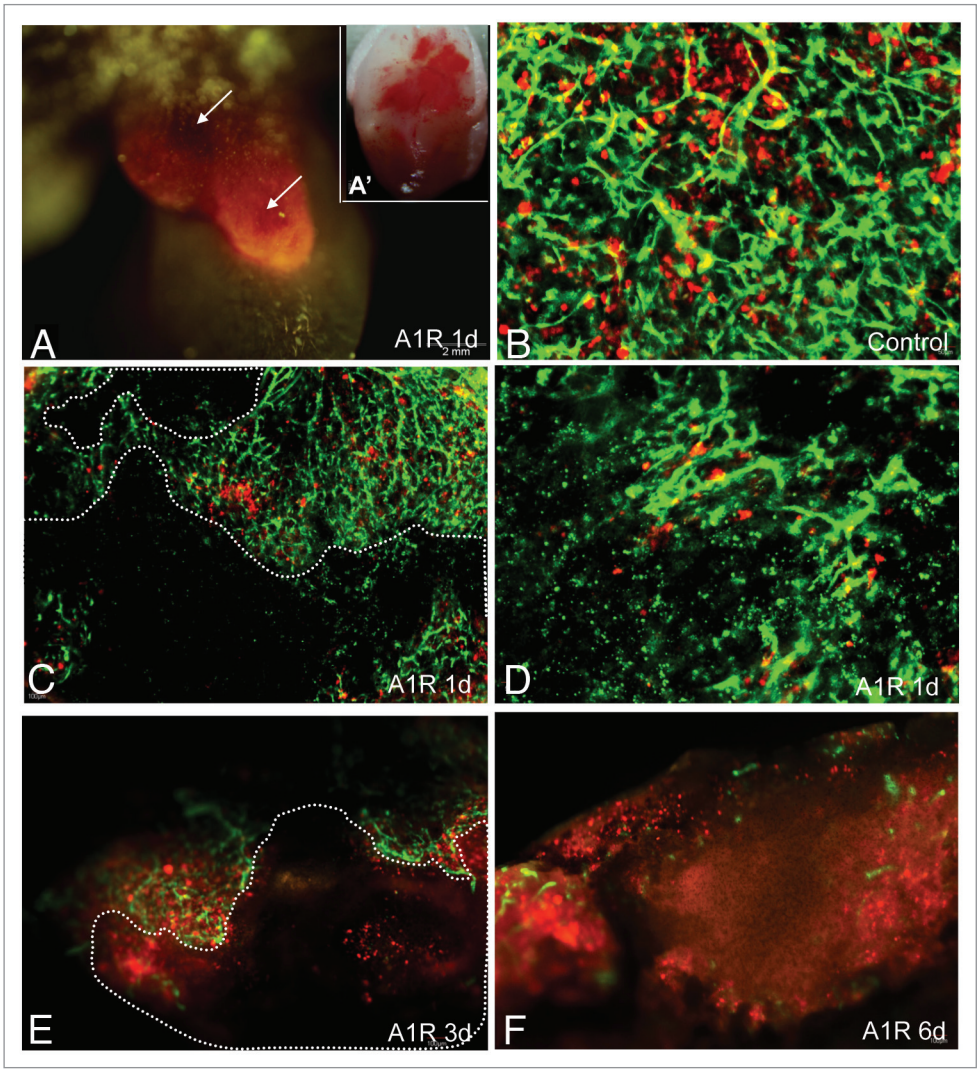

Figure 4. Bacteria-induced tumor blood vessel destruction in the ear. LLC-RFP tumors were implanted in the ear of ND-GFP mice (A and A'). Tumors were observed with the Olympus OV100 imaging system at day 1 after A1-R injection. (A) LLC-RFP tumor with red fluorescence. Hemorrhagic areas were near the skin surface. (A') The tumor was excised, and severe hemorrhage is seen under brightfield (B–F). Tumors were observed with the Olympus IV100 imaging system. Blood vessels expressed GFP and LLC expressed RFP. Dashed lines show damaged blood vessel areas. Most blood vessels were destroyed by day 1 after A1-R bacteria injection. Only a small area of the tumor remained by day 3. By day 6, just a few blood vessels remained.

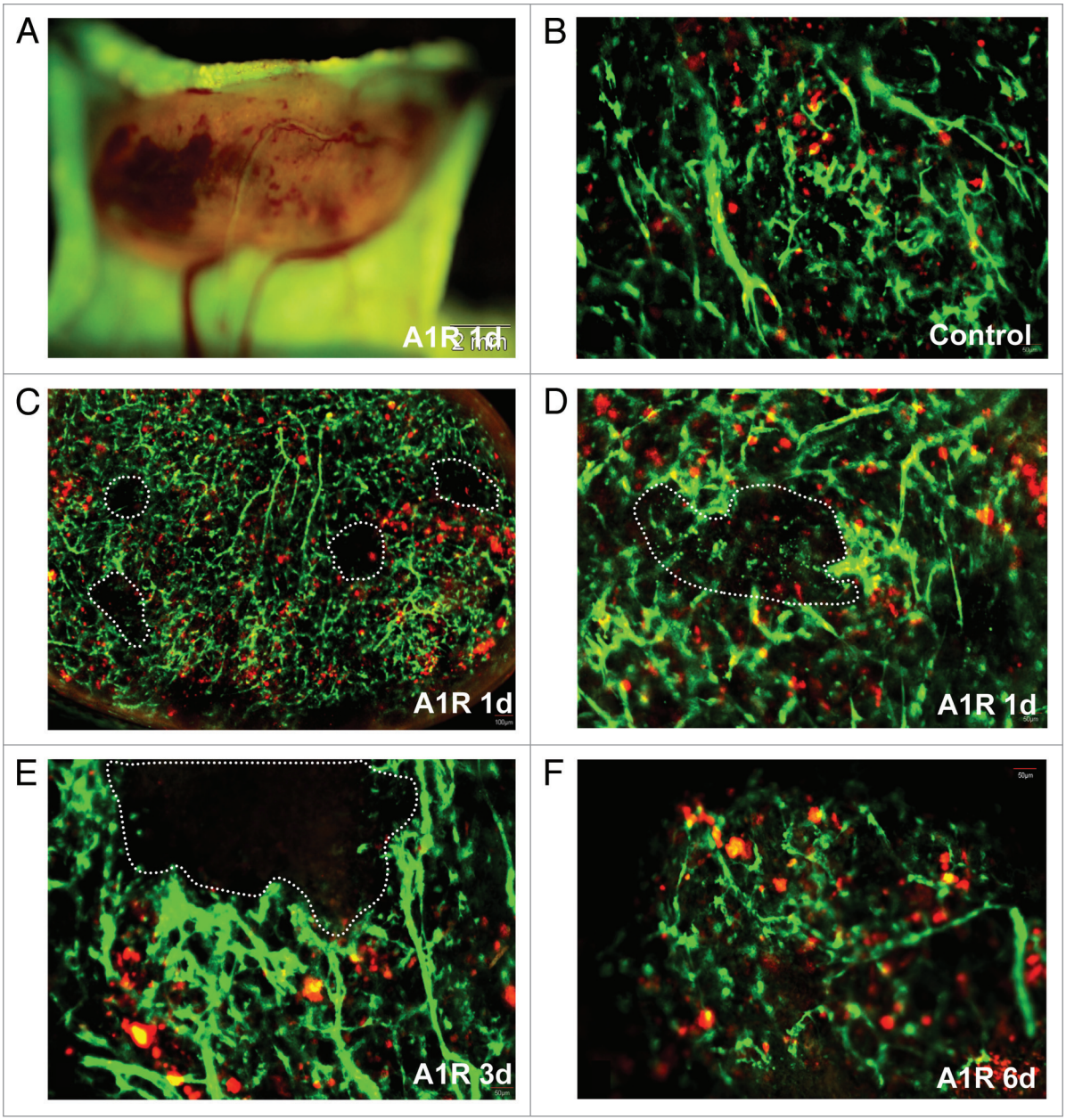

Figure 5. Bacteria-induced tumor blood vessel destruction in the back. (A) was observed with the Olympus OV100 imaging system. Tumors hemorrhaged near the surface (B–F). Tumors were observed with the Olympus IV100 imaging system. Blood vessels expressed GFP and LLC expressed RFP. Dashed lines show damaged blood vessel areas. In some small areas, tumor blood vessels were damaged at day 1 after A1-R bacteria injection. At days 3 and 6, more blood vessels were damaged.

Leschner et al. reported that *Salmonella enterica* serovar Typhimurium colonization of solid tumors was accompanied by hemorrhage promoted by TNFα.[29] In the present study, we observed that after day 1 of A1-R bacteria infection, the hemorrhage of the ear and back tumors was found, but the foot tumor had no hemorrhage. This site difference of hemorrhage suggests that there is some other mechanism of tumor sensitivity to *S. typhimurium* besides TNFα.

Results of the present study demonstrate an important advantage of the use of a facultative anaerobe, such as *S. typhimurium*, over obligate anaerobes, such as Clostridia[16] or Bifidobacteria,[14,15] which are confined to the anaerobic regions of tumors and therefore, cannot target its vascular system.

Our results suggest that tumor vascularity influences the efficacy of A1-R bacteria. In future studies, *S. typhimurium* A1-R will be targeted to highly vascular tumors in order to improve efficacy.

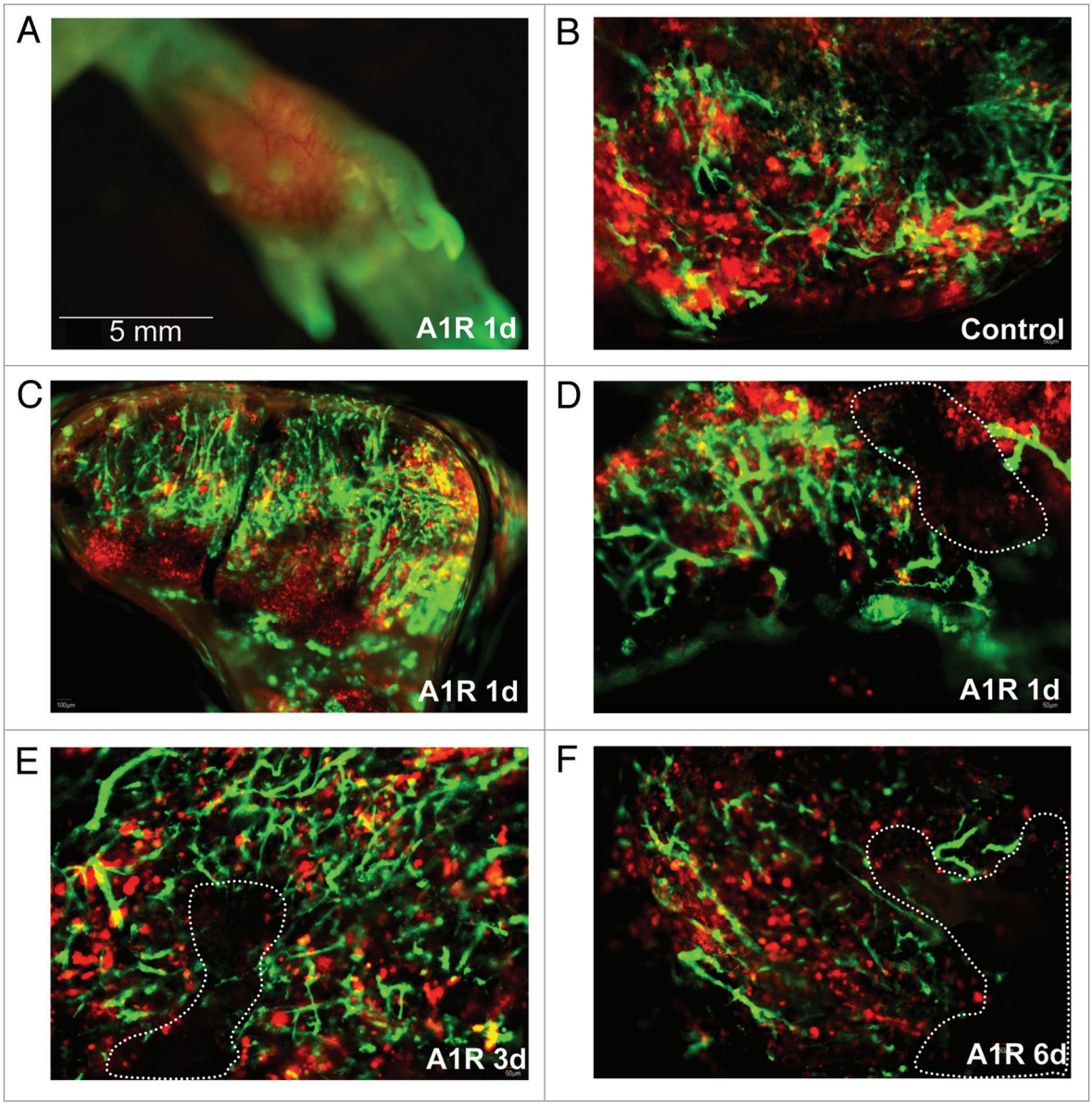

Figure 6. Bacteria-induced tumor blood vessel destruction in the footpad. (A) was observed with the Olympus OV100 imaging system. No hemorrhage was found at the surface of the tumor. (B~F) were observed with the Olympus IV100 imaging system. Blood vessels expressed GFP and LLC expressed RFP. Dashed lines showed damaged blood vessel areas. A small area of tumor blood vessels was damaged at day 1 after A1-R bacteria injection. At day 6, blood vessels were largely destroyed.

Materials and Methods

ND-GFP transgenic nude mice. ND-GFP transgenic C57/B6 mice express GFP under control of nestin regulatory elements.[32,33] Previously, the ND-GFP gene had been crossed into nude mice with the C57/B6 background, to obtain ND-GFP nude mice.[31,34]

Preparation of RFP Lewis lung cancer cells (LLCs). LLCs murine cancer cells labeled with RFP were recovered and passaged in cell culture flasks by conventional culture methods. After two or three successive passages, cells were collected for injection. The cell density was 2 x 10^7 cells per milliliter.

RFP-expressing murine cutaneous lung cancer model. Ten nestin-GFP transgenic nude mice, six to eight weeks old, were used. The mice were anesthetized with tribromoethanol [i.p. injection (0.2 mL/10 g body weight) of a 1.2% solution]. RFP-expressing LLC murine lung cancer cells (2 x 10^7 cells/ml) were injected into the skin of the ear, back and footpad of the ND-GFP nude mice with a 1 mL 27G1/2 latex-free syringe at 25 μl each site.

CD31-immunohistochemical staining. After ten days of tumor growth, the tumors at different sites were harvested. Frozen sections were made. Slides were fixed with 4% precool paraformaldehyde. The main staining protocol was as follows: endogenous peroxidase activity was blocked by incubating the slides in 0.3% H_2O_2 solution in PBS for 10 minutes and incubated with the rat CD31 antibody (1:10) at 4°C overnight. The

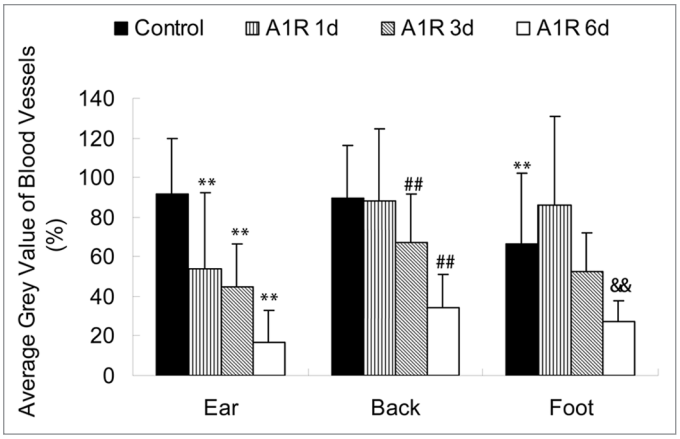

Figure 7. Average grey value of the Lewis lung tumor blood vessels at different body sites. The average grey value of the foot tumor blood vessels was less than that in the ear tumor blood vessels ($p < 0.05$). The average grey value of blood vessels in the ear tumor decreased at days 1, 3 and 6 after A1-R bacteria treatment ($p < 0.01$). In the back tumor, the average grey value of blood vessels at days 3 and 6 after bacterial treatment showed decreases ($p < 0.01$). In the foot tumor, the average grey value of blood vessels at day 6 was significantly decreased ($p < 0.01$). Imaging was done with the FluorVivo imaging system (INDEC Biosystems). **$p < 0.01$ vs. ear tumor control group; ##$p < 0.01$ vs. back tumor control group; &&$p < 0.01$ vs. foot tumor control group.

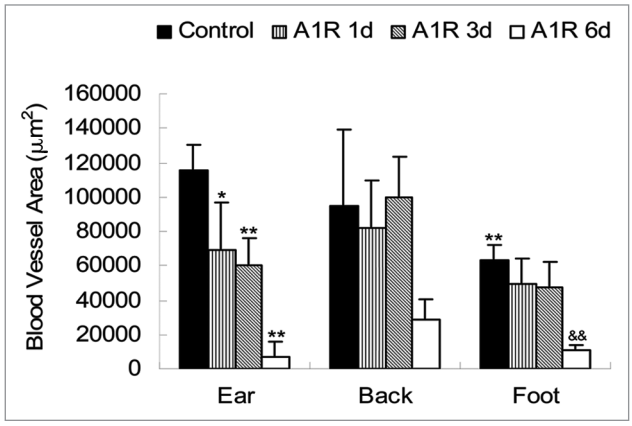

Figure 8. Blood vessel area of the Lewis lung tumor at different body sites. The blood vessel area of the foot tumor was less than that in the ear tumor ($p < 0.01$). The blood vessel area in the ear tumor decreased at day 1 ($p < 0.05$) and even more severely at days 3 and 6 after A1-R bacteria treatment ($p < 0.01$). The back tumor had no significant change in the blood vessel area, since the blood vessel fragments did not disappear soon after damage. In the foot pad tumor, the blood vessel area at day 6 after A1-R treatment was significantly decreased ($p < 0.01$). Imaging was done with the FluorVivo imaging system (INDEC Biosystems). **$p < 0.01$ vs. ear tumor control group; &&$p < 0.01$ vs. foot tumor control group.

biotinylated anti-Ig secondary antibody (1:50), was incubated for 30 minutes at room temperature. Streptravidin-HRP was applied to the tissue sections for 30 minutes at room temperature. The DAB color agent was applied for 5 minutes at room temperature. Slides were counterstained in hematoxylin solution for 60 seconds, dehydrated, cleared and cover-slipped.

Evaluation of the density of the Lewis lung tumor cells at different sites. The cell numbers of ten random areas (1 mm^2 each) was counted in tissue sections made from each tumor site. The average tumor cell number per mm^2 at different sites were obtained and compared.

Preparation of the modified A1-R strain of *Salmonella typhimurium*. A1-R bacteria were grown overnight on LB medium and then diluted 1:10 in LB medium. Bacteria were harvested at late-log phase, washed with PBS, and then diluted in PBS. Bacteria were then injected into the tail vein of nude mice (5×10^7 cfu per 100 μl PBS).[35]

AI-R treatment of tumor. Ten days after tumor growth, the tumor-bearing nestin-GFP mice were treated with AI-R bacteria (5×10^7) via tail-vein injection. Mice without A1-R injection served as untreated controls.

Small-animal imaging systems. The Olympus OV100 Small Animal Imaging System (Olympus Corp., Tokyo, Japan), containing an MT-20 light source (Olympus Biosystems, Planegg, Germany) and DP70 CCD camera (Olympus), was used for subcellular imaging in live mice. The optics of the OV100 fluorescence imaging system have been specially developed for macroimaging as well as microimaging with high light-gathering capacity. The instrument incorporates a unique combination of high numerical aperture and long working distance. Individually optimized objective lenses, parcentered and parfocal, provide a 105-fold magnification range for seamless imaging of the entire body down to the subcellular level without disturbing the animal. The OV100 has lenses mounted on an automated turret with a high magnification range of x1.6 to x16 and a field of view ranging from 6.9 to 0.69 mm. The optics and anti-reflective coatings ensure optimal imaging of multiplexed fluorescent reporters in small animals. High-resolution images were captured directly on a PC (Fujitsu Siemens, Munich, Germany). Images were processed for contrast and brightness and analyzed with the use of Paint Shop Pro 8 and Cell®.[36]

Laser scanning microscope. The Olympus IV100 microscope is a scanning laser microscope. A 488 nm argon laser was used. The novel stick objectives (as small as 1.3 mm) were designed specifically for this laser scanning microscope. The very narrow objectives deliver very high resolution images. A PC computer running FluoView software (Olympus Corp.) was used to control the microscope. All images were recorded and stored as proprietary multilayer 16-bit Tagged Image File Format files.[37]

Statistical analysis. Images were processed for area evaluation of tumor blood vessels with the use of FluorVivo Mag software (INDEC Biosystems) and average grey value of tumor blood vessels with the use of Paint Shop Pro 8 and Cell (Olympus). The experimental data are expressed as the mean ± SD. Statistical analysis was done using two-tailed Student's t test.

Acknowledgements

This study was supported by the US Army Medical Research and Materiel Command Prostate Cancer Research Program Award W81XWH-06-1-0117 and W81XWH-08-1-0719 and National Institutes of Health Grants CA119841 and CA126023.

References

1. Coley WB. Late results of the treatment of inoperable sarcoma by the mixed toxins of erysipelas and Bacillus prodigiosus. Am J Med Sci 1906; 131:375-430.
2. Malmgren RA, Flanigan CC. Localization of the vegetative form of *Clostridium tetani* in mouse tumors following intravenous spore administration. Cancer Res 1955; 15:473-8.
3. Gericke D, Engelbart K. Oncolysis by clostridia. II. Experiments on a tumor spectrum with a variety of clostridia in combination with heavy metal. Cancer Res 1964; 24:217-21.
4. Moese JR, Moese G. Oncolysis by clostridia. I. Activity of *Clostridium butyricum* (M_{55}) and other nonpathogenic clostridia against the Ehrlich carcinoma. Cancer Res 1964; 24:212-6.
5. Thiele EH, Arison RN, Boxer GE. Oncolysis by clostridia. III. Effects of clostridia and chemotherapeutic agents on rodent tumors. Cancer Res 1964; 24:222-33.
6. Kohwi Y, Imai K, Tamura Z, Hashimoto Y. Antitumor effect of *Bifidobacterium infantis* in mice. Gann 1978; 69:613-8.
7. Kimura NT, Taniguchi S, Aoki K, Baba T. Selective localization and growth of *Bifidobacterium bifidum* in mouse tumors following intravenous administration. Cancer Res 1980; 40:2061-8.
8. Fox ME, Lemmon MJ, Mauchline ML, Davis TO, Giaccia AJ, Minton NP, et al. Anaerobic bacteria as a delivery system for cancer gene therapy: in vitro activation of 5-fluorocytosine by genetically engineered clostridia. Gene Ther 1996; 3:173-8.
9. Lemmon MJ, Van Zijl P, Fox ME, Mauchline ML, Giaccia AJ, Minton NP, et al. Anaerobic bacteria as a gene delivery system that is controlled by the tumor microenvironment. Gene Ther 1997; 4:791-6.
10. Brown JM, Giaccia AJ. The unique physiology of solid tumors: opportunities (and problems) for cancer therapy. Cancer Res 1998; 58:1408-16.
11. Low KB, Ittensohn M, Le T, Platt J, Sodi S, Amoss M, et al. Lipid A mutant *Salmonella* with suppressed virulence and TNFα induction retain tumor-targeting in vivo. Nat Biotechnol 1999; 17:37-41.
12. Clairmont C, Lee KC, Pike J, Ittensohn M, Low KB, Pawelek J, et al. Biodistribution and genetic stability of the novel antitumor agent VNP20009, a genetically modified strain of *Salmonella typhimurium*. J Infect Dis 2000; 181:1996-2002.
13. Sznol M, Lin SL, Bermudes D, Zheng LM, King I. Use of preferentially replicating bacteria for the treatment of cancer. J Clin Invest 2000; 105:1027-30.
14. Yazawa K, Fujimori M, Amano J, Kano Y, Taniguchi S. *Bifidobacterium longum* as a delivery system for cancer gene therapy: selective localization and growth in hypoxic tumors. Cancer Gene Ther 2000; 7:269-74.
15. Yazawa K, Fujimori M, Nakamura T, Sasaki T, Amano J, Kano Y, et al. *Bifidobacterium longum* as a delivery system for gene therapy of chemically induced rat mammary tumors. Breast Cancer Res Treat 2001; 66:165-70.
16. Dang LH, Bettegowda C, Huso DL, Kinzler KW, Vogelstein B. Combination bacteriolytic therapy for the treatment of experimental tumors. Proc Natl Acad Sci USA 2001; 98:15155-60.
17. Hoiseth SK, Stocker BA. Aromatic-dependent *Salmonella typhimurium* are non-virulent and effective as live vaccines. Nature 1981; 291:238-9.
18. Pawelek JM, Low KB, Bermudes D. Tumor-targeted Salmonella as a novel anticancer vector. Cancer Res 1997; 57:4537-44.
19. Toso JF, Gill VJ, Hwu P, Marincola FM, Restifo NP, Schwartzentruber DJ, Sherry RM, et al. Phase I study of the intravenous administration of attenuated *Salmonella typhimurium* to patients with metastatic melanoma. J Clin Oncol 2002; 20:142-52.
20. Mengesha A, Dubois L, Lambin P, Landuyt W, Chiu RK, Wouters BG, et al. Development of a flexible and potent hypoxia-inducible promoter for tumor-targeted gene expression in attenuated Salmonella. Cancer Biol Ther 2006; 5:1120-8.
21. Yu YA, Timiryasova T, Zhang Q, Beltz R, Szalay AA. Optical imaging: bacteria, viruses and mammalian cells encoding light-emitting proteins reveal the locations of primary tumors and metastases in animals. Anal Bioanal Chem 2003; 377:964-72.
22. Yu YA, Shabahang S, Timiryasova TM, Zhang Q, Beltz R, Gentschev I, Goebel, et al. Visualization of tumors and metastases in live animals with bacteria and vaccinia virus encoding light-emitting proteins. Nat Biotechnol 2004; 22:313-20.
23. Zhao M, Yang M, Li XM, Jiang P, Baranov E, Li S, et al. Tumor-targeting bacterial therapy with amino acid auxotrophs of GFP-expressing *Salmonella typhimurium*. Proc Natl Acad Sci USA 2005; 102:755-60.
24. Zhao M, Yang M, Ma H, Li X, Tan X, Li S, et al. Targeted therapy with a *Salmonella typhimurium* leucine-arginine auxotroph cures orthotopic human breast tumors in nude mice. Cancer Res 2006; 66:7647-52.
25. Hayashi K, Zhao M, Yamauchi K, Yamamoto N, Tsuchiya H, Tomita K, et al. Systemic targeting of primary bone tumor and lung metastasis of high-grade osteosarcoma in nude mice with a tumor-selective strain of *Salmonella typhymurium*. Cell Cycle 2009; 8:870-5.
26. Hayashi K, Zhao M, Yamauchi K, Yamamoto N, Tsuchiya H, Tomita K, et al. Cancer metastasis directly eradicated by targeted therapy with a modified *Salmonella typhymurium*. J Cell Biochem 2009; 106:992-8.
27. Nagakura C, Hayashi K, Zhao M, Yamauchi K, Yamamoto N, Tsuchiya H, et al. Efficacy of a genetically-modified *Salmonella typhimurium* in an orthotopic human pancreatic cancer in nude mice. Anticancer Res 2009; 29:1873-8.
28. Yam C, Zhao M, Hayashi K, Ma H, Kishimoto H, McElroy M, et al. Monotherapy with a tumor-targeting mutant of *S. typhimurium* inhibits liver metastasis in a mouse model of pancreatic cancer. J Surg Res 2009; 164:248-55.
29. Leschner S, Westphal K, Dietrich N, Viegas N, Jablonska J, Lyszkiewicz M, et al. Tumor invasion of *Salmonella enterica* serovar Typhimurium is accompanied by strong hemorrhage promoted by TNFα. PLoS One 2009; 4:e6692.
30. Amoh Y, Li L, Yang M, Jiang P, Moossa AR, Katsuoka K, et al. Hair follicle-derived blood vessels vascularize tumors in skin and are inhibited by doxorubicin. Cancer Res 2005; 65:2337-43.
31. Amoh Y, Yang M, Li L, Reynoso J, Bouvet M, Moossa AR, et al. Nestin-linked green fluorescent protein transgenic nude mouse for imaging human tumor angiogenesis. Cancer Res 2005; 65:5352-7.
32. Li L, Mignone J, Yang M, Matic M, Penman S, Enikolopov G, et al. Nestin expression in hair follicle sheath progenitor cells. Proc Natl Acad Sci USA 2003; 100:9958-61.
33. Amoh Y, Li L, Yang M, Moossa AR, Katsuoka K, Penman S, et al. Nascent blood vessels in the skin arise from nestin-expressing hair follicle cells. Proc Natl Acad Sci USA 2004; 101:13291-5.
34. Hayashi K, Yamauchi K, Yamamoto N, Tsuchiya H, Tomita K, Bouvet M, et al. A color-coded orthotopic nude-mouse treatment model of brain-metastatic paralyzing spinal cord cancer that induces angiogenesis and neurogenesis. Cell Proliferation 2009; 42:75-82.
35. Zhao M, Geller J, Ma H, Yang M, Penman S, Hoffman RM. Monotherapy with a tumor-targeting mutant of *Salmonella typhimurium* cures orthotopic metastatic mouse models of human prostate cancer. Proc Natl Acad Sci USA 2007; 104:10170-4.
36. Yamauchi K, Yang M, Jiang P, Xu M, Yamamoto N, Tsuchiya H, et al. Development of real-time subcellular dynamic multicolor imaging of cancer-cell trafficking in live mice with a variable-magnification whole-mouse imaging system. Cancer Res 2006; 66:4208-14.
37. Yang M, Jiang P, Hoffman RM. Whole-body subcellular multicolor imaging of tumor-host interaction and drug response in real time. Cancer Res 2007; 67:5195-200.